

The Evaporative Fraction as a Measure of Surface Energy Partitioning

W. E. Nichols

Geosciences Department, Pacific Northwest Laboratory, Richland, Washington

R. H. Cuenca

Department of Bioresource Engineering, Oregon State University, Corvallis, Oregon

Short Title: Evaporative Fraction

DISCLAIMER

This report was prepared as an account of work sponsored by an agency of the United States Government. Neither the United States Government nor any agency thereof, nor any of their employees, makes any warranty, express or implied, or assumes any legal liability or responsibility for the accuracy, completeness, or usefulness of any information, apparatus, product, or process disclosed, or represents that its use would not infringe privately owned rights. Reference herein to any specific commercial product, process, or service by trade name, trademark, manufacturer, or otherwise does not necessarily constitute or imply its endorsement, recommendation, or favoring by the United States Government or any agency thereof. The views and opinions of authors expressed herein do not necessarily state or reflect those of the United States Government or any agency thereof.

DISTRIBUTION OF THIS DOCUMENT IS UNLIMITED

MASTER

Abstract

The evaporative fraction is a ratio that expresses the proportion of turbulent flux energy over land surfaces devoted to evaporation and transpiration (evapotranspiration). It has been used to characterize the energy partition over land surfaces and has potential for inferring daily energy balance information based on mid-day remote sensing measurements. The HAPEX-MOBILHY program's SAMER system provided surface energy balance data over a range of agricultural crops and soil types. The database from this large-scale field experiment was analyzed for the purpose of studying the behavior and daylight stability of the evaporative fraction in both ideal and general meteorological conditions. Strong linear relations were found to exist between the mid-day evaporative fraction and the daylight mean evaporative fraction. Statistical tests however rejected the hypothesis that the two quantities were equal. The relations between the evaporative fraction and the surface soil moisture as well as soil moisture in the complete vegetation root zone were also explored.

Introduction

The HAPEX-MOBILHY Program

The HAPEX-MOBILHY (Hydrologic Atmospheric Pilot Experiment - Modélization du Bilan Hydrique) Program was directed at the study of the hydrologic budget and evaporation flux at the scale of a General Circulation Model (GCM) grid cell, i.e., 10^4 km² [André et al., 1986; André et al., 1988]. The experiment area was a grid 100 km by 100 km made up of the Leyre and Adour River drainage basins situated between Toulouse and Bordeaux in southwest France. Major climatic influences included the Pyrennes Mountains (65 km south of the grid) and the Atlantic Ocean. Land use in the grid consisted of approximately 60% agricultural crop land and 40% forest. Major crops included maize, pasture, orchards, and vineyards. The forested area was the man-planted Landes Forest in the northern portion of the grid. There were cultivated agricultural clearings of various sizes within the forested area.

Different surface and subsurface measurement networks were operated in this grid from mid-1985 through early 1987 to monitor soil moisture, surface energy flux, surface hydrology, and atmospheric properties. A Special Observing Period (SOP) was conducted from May 7 to July 15, 1986, and included measurement of surface energy balance terms using a mesoscale network of SAMER (Système Automatique de Mesure de l'Evapotranspiration Réelle) stations [Bessemoulin et al., 1986]. In addition, soil moisture at depth was monitored using a neutron probe at 14 locations in the HAPEX-MOBILHY grid, 12 of which coincided with the SAMER station locations. This paper draws on the extensive SAMER and neutron probe data collected during this large-scale field experiment to examine the behavior and daytime stability of the evaporative fraction.

The Evaporative Fraction

The energy balance of the Earth's surface can be assumed to be comprised of four major

fluxes: net radiation, soil heat flux, sensible heat flux, and latent heat flux. Net radiation is the energy available at the Earth's surface derived from absorbed solar and terrestrial radiation. Net radiation is taken as positive when absorbed radiation components exceed emitted and reflected components. Soil heat flux is energy transfer between the ground and the Earth's surface, taken as positive when the soil is warming. Sensible heat flux is energy transfer between the atmosphere and Earth's surface not associated with water vapor transport, taken as positive when the atmosphere is warming. Finally, latent heat flux is energy transfer between the surface and the atmosphere that is associated with water vapor transport, taken as positive when water vapor is transported from the surface to the atmosphere. The mathematical relationship encompassing these four components is given by the surface energy balance equation

$$R_N = \lambda E + H + G \quad (1)$$

where R_N is the net radiation ($W m^{-2}$), λ is the latent heat of evaporation or condensation (approximately $2.45 \times 10^3 J g^{-1}$ at $20^\circ C$), E is the evaporation or condensation rate ($g m^{-2} s^{-1}$), H is the sensible heat flux ($W m^{-2}$), and G is the soil heat flux ($W m^{-2}$). The product λE is the latent heat flux ($W m^{-2}$).

The evaporative fraction is defined as the ratio of latent heat flux to the sum of latent and sensible heat fluxes:

$$EF = \frac{\lambda E}{\lambda E + H} \quad (2)$$

where all terms are as defined previously for Equation (1). The evaporative fraction has been used by FIFE (First ISLSCP Field Experiment; ISLSCP is the International Satellite Land Surface Climatology Program) researchers to characterize the surface energy balance over the FIFE Program area. The FIFE program involved detailed study of land surface processes over a 15-km

by 15-km grassland area in the Konza Prairie Reserve, Kansas. The objective of the program was to determine which land surface parameters could be determined from remotely sensed data [Sellers et al. 1989]. Shuttleworth et al. [1989] found a strong linear correlation between the value of the evaporative fraction at mid-day and the daytime average value for the four "golden days" of the FIFE Intensive Field Campaigns (IFCs) in 1987. This result was considered useful because it implied that the daytime average evaporative fraction was a quantity that could be adequately deduced from a single, instantaneous remote sensing measurement [Shuttleworth et al., 1989].

Measurements

The SAMER network consisted of 12 stations scattered through the HAPEX-MOBILHY grid as shown in Figure 1. The 12 stations are listed in Table 1 with each station's identity number, location, elevation, crop cover, soil texture, and irrigation status. All 12 stations were operated by the Centre National de Recherches Météorologiques, Toulouse, France.

The SAMER system applied the surface energy balance equation [Equation (1)] to compute latent heat flux as a residual. Net radiation was directly measured with a net radiometer. A buried flux-meter was used to measure soil heat flux. A simplified aerodynamic method was used to determine the sensible heat flux from measurements of the wind speed and temperature differentials between two levels above the crop canopy. The sensors used and the data collected by the SAMER system are listed in Table 2. All parameters except precipitation were averaged over 15-min intervals. Precipitation was recorded as a cumulative value for 15-min intervals. In Table 2, "basic measurements" are those parameters required to compute the latent heat flux as a residual with Equation (1), and "other measurements" are those data collected that were not required for computation of the latent heat flux.

The simplified aerodynamic formula applied by the SAMER system was developed by Itier [1980; 1982] and Riou [1982]. Measurements of wind speed and dry bulb air temperature at two levels above the canopy were required to compute the sensible heat flux. The first step in this method was to compute the dimensionless Richardson Number (R_i) to determine the thermal stability of the lower atmosphere:

$$R_i = \left(\frac{g}{T_a} \right) (z_2 - z_1)^{1/2} \log \left(\frac{z_2}{z_1} \right) \left[\frac{\Delta T}{(\Delta V)^2} \right] \quad (3)$$

where g is the acceleration due to gravity (m s^{-2}), T_a is the air temperature, and ΔT and ΔV are the temperature ($^{\circ}\text{C}$) and wind velocity (m s^{-1}) differentials, respectively, between two probes at

measurement heights z_1 and z_2 (m). Next, the sensible heat flux for neutral conditions was computed from

$$H_0 = \frac{\rho C_p \kappa^2}{\left[\log\left(\frac{z_2}{z_1}\right)\right]^2} \Delta T \Delta V \quad (4)$$

where ρ is the air density, C_p is the specific heat capacity, and κ is the von Karman constant (≈ 0.38 , dimensionless). Finally, the sensible heat flux was computed from one of four equations, depending on the value of the Richardson number;

$$H = \frac{1.3 \rho C_p \left(\frac{g}{T}\right)^{1/2} \Delta T^{3/2}}{\left[3 \left(z_1^{1/3} z_2^{1/3}\right)\right]^{3/2}} \quad R_i < -1 \quad (5(a))$$

$$H = H_0 (1 - 16 R_i)^{3/4} \quad -1 < R_i < 0 \quad (5(b))$$

$$H = H_0 (1 - 5 R_i)^2 \quad 0 < R_i < 0.14 \quad (5(c))$$

$$H = \frac{H_0}{10} \quad 0.14 < R_i \quad (5(d))$$

The network of SAMER stations provided a useful ground data set against which remote sensing methods could be developed, calibrated, and tested. It is important to consider the precision with which the SAMER stations measured surface energy fluxes in analyzing these data. Goutorbe [1990] reported on benchmark studies for the equipment and identified the principal errors expected from SAMER data collected during the SOP. Relative uncertainty in an individual 15-min sensible heat flux estimate depended on atmospheric stability but could be as high as

20%. This error could be reduced by approximately one-half by using daily averages instead of 15-min values. Another important error for analysis of short-term fluxes was net radiation, which was underestimated by 5% to 10% during peak periods of clear days [Marre and Goutorbe, 1988]. Unpublished corrections to net radiation based on incoming solar radiation at each SAMER site have been developed but were not available at the time analyses were conducted for this article. Goutorbe [1990] concluded that, taken together, the result of instrumental measurement errors caused the SAMER stations to be incapable of differentiating surface fluxes differing by less than 15% to 20%. Nevertheless, review of all daily fluxes conducted as part of this study indicated an impressive response of SAMER measured fluxes to canopy development, periods following precipitation, and crop maturity.

Results

Diurnal Behavior of the Evaporative Fraction

The evaporative fraction was found by FIFE investigators to be a relatively stable and therefore useful tool for characterization of the relative energy partition [Sellers et al., 1989; Shuttleworth et al., 1989]. This study applies a different database collected in the HAPEX-MOBILHY program to further study the behavior of the mid-day evaporative fraction relative to the daily evaporative fraction.

FIFE investigators examined the behavior of the evaporative fraction for the four "golden days" of the FIFE program's four 1987 IFCs. For fairly ideal conditions, i.e., no clouds and a "typical" sinusoidal surface energy balance, the evaporative fraction was relatively stable. This paper examines whether this stability holds for less ideal conditions. The SAMER database was examined for both "clear-sky" and for more general non-precipitation conditions.

The diurnal surface energy balance measured at the SAMER 01 station (Lubbock 1) on June 16, 1986, is shown in Figure 2. This station was located in a mature oat field. The high transpiration rate for the oat canopy is reflected in the proportion of latent heat flux. A very different partitioning of surface energy is observed in an adjacent field covered with young maize approximately 10-cm in height (Figure 3). In this field the latent heat flux is a much less dominant part of the energy balance, while the soil heat flux and sensible heat flux both represent a greater portion of available energy. These figures illustrate that even for significantly different crop conditions the predominant energy transfer in a 24-hour period occurs during the daylight hours in response to solar radiation. Night fluxes are much smaller in magnitude and do not have much impact on the total daily energy balance. For example, the ratio of day to night absolute latent heat flux for the 24-hour period shown in Figure 2 is 10.8 to 1.0, while for the same period shown in Figure 3 this ratio is 10.6 to 1.0.

The evaporative fraction is computed as a ratio of latent heat flux over the sum of latent

and sensible heat flux exchanged between the atmosphere and the land surface. At night these fluxes are relatively small in magnitude and typically undergo sign reversal. Consequently, the evaporative fraction is highly unstable at night and possibly undefined (division by zero). For this reason, any analysis of the evaporative fraction is necessarily restricted to daylight periods. Little information is lost by neglecting the night hours for the reasons discussed above.

The evaporative fraction profiles for the surface energy balance data collected by SAMER 01 and SAMER 05 (Figures 2 and 3, respectively) are depicted in Figure 4. The evaporative fraction for SAMER 01 is consistently higher than for SAMER 05, reflecting the greater transpiration activity in the oat field for that day. The "nominal daylight period" is indicated in Figure 4 to show the approximate daylight period for June 16, 1986. The instability of the evaporative fraction at night was often found to occur near the sunrise and sunset periods. Because of this instability, the evaporative fraction was only considered in this study for the periods beginning 1-hour after sunrise until 1-hour prior to sunset.

Computation of the Evaporative Fraction

The SAMTRAN computer program was developed to expedite data management and analysis for the large HAPEX-MOBILHY SAMER database [Nichols, 1989b]. The evaporative fraction was computed using this program for each available 15-min record and stored along with corresponding surface energy balance data. Since only the daylight period was of interest, SAMTRAN was coded to store this information only for the period beginning 1-hour after sunrise until 1-hour prior to sunset. Local sunrise and sunset times were computed in SAMTRAN using the following set of equations from the British Meteorological Office MORECS model [Thompson et al., 1981]:

$$t_1 = \left(\frac{12}{\pi}\right) \cos^{-1} \left[\tan(\delta) \tan(\phi) + \left(\frac{0.0145}{\cos(\delta) \cos(\phi)}\right) \right] \quad (6)$$

$$t_2 = 24 - t_1 \quad (7)$$

$$\delta = 0.41 \cos \left[2\pi \left(\frac{N - 172}{365} \right) \right] \quad (8)$$

where t_1 and t_2 are the sunrise and sunset times in hours respectively, ϕ is the latitude in decimal degrees, N is the day of the year (or Julian date), and δ is the solar declination angle in radians.

The surface energy balance and precipitation data were examined graphically to classify the dates. If precipitation was recorded for more than one 15-min interval in a day, that date was removed from further consideration. This exclusion was made to avoid those dates in which the surface energy balance was complicated by precipitation. If any of the three measured surface energy balance terms (net radiation, sensible heat flux, and soil heat flux) were not continuously recorded during the daylight period, that date was also removed from the set. The remaining dates were classified as either "clear-sky" or "non-clear-sky" based on the graphical appearance of the diurnal surface energy balance. A smooth sinusoidal pattern was evidence of the first class, while deviations from that pattern resulted in the latter class. Although nominally subjective, this classification scheme was introduced to permit analysis of data for ideal conditions in contrast to more general meteorological conditions. By way of example, the surface energy balances shown in Figures 2 and 3 were classified as clear-sky while Figure 5 represents a station and date (Fusterouau, SAMER 11, June 4, 1986) classified as non-clear-sky. Non-clear-sky conditions predominated in the semi-humid climate of the HAPEX-MOBILHY grid during the SOP. Of the 453 station-dates available, 91 were classified as clear-sky.

The mean mid-day evaporative fractions were computed for the accepted data from the 15-min interval records between 1100 hours and 1300 hours LT (local time). This corresponds to the time period when most land surface remote sensing missions are flown. The all-day evaporative fraction was computed from the daylight period exclusive of the mid-day period. The

exclusion of the records used to compute the mid-day evaporative fraction was necessary to prevent auto-correlation and to maintain independence of the statistics. For data classified as clear-sky, the mid-day and all-day evaporative fractions were saved to both a general data set and clear-sky data set. For data classified as non-clear-sky, these statistics were saved only to the general data set.

Evaporative Fraction Stability

Figure 6a-l shows 12 scatter plots of the mid-day evaporative fraction versus the corresponding all-day evaporative fraction for the 12 SAMER stations. In each figure the clear-sky classified data are represented by circles (o), while non-clear-sky data are represented by plus symbols (+). The 1:1 line (X=Y line) is shown as dashed. The solid line depicted in each plot is the linear least-squares regression fit to the general set (all points) for the respective station. Figure 7 shows all clear-sky data from the twelve SAMER stations. The strong correlation for ideal conditions noted by FIFE researchers is evident in Figure 7. For the more general cases (Figure 6a-l), the correlation does not appear as well defined. The strength of the linear relationship was always greater for the clear-sky data set than for the general data set at every site and for the experiment as a whole. Linear regression statistics are summarized in Table 3. The notation used in Table 3 follows a simple linear regression equation written as

$$Y = \beta_0 + \beta_1 X \quad (9)$$

where X is the independent variable, Y is the dependent variable, β_0 is the Y axis intercept, and β_1 is the slope of the least-squares regression line [Weisberg, 1985]. Statistical error components were not included in Equation (9) for clarity purposes; a review of the full simple regression model is not required for this discussion. The coefficient of determination summary statistic, which describes the strength of the relationship between X and Y in the data, is denoted by r^2

[Weisberg, 1985]. The number of samples or observations is denoted by n .

Statistical inference was used to determine if the evaporative fraction measured at mid-day was representative of the daylight period. The statistical question posed is whether the all-day evaporative fraction was equal to the mid-day evaporative fraction, or equivalently, whether the mean of the difference in these statistics was equal to zero. The statistics are paired by nature, permitting use of the paired-t test if the approximate normality assumption is met with respect to the distribution of the differences. Based on the relatively large sample size (38 samples per station on average) and examination of normal probability plots, the approximate normality assumption appeared valid.

The paired-t test was used for both the clear-sky and general data sets. The hypothesis for the test is formally constructed as follows [Devore and Peck, 1986]:

$$H_0: \mu_d = \mu_1 - \mu_2 = 0 \quad (\text{null hypothesis})$$

$$H_a: \mu_d \neq 0 \quad (\text{alternative hypothesis})$$

which is a two-tailed test. In this statistical notation, μ_1 and μ_2 are the true but unknown mean values estimated by the two statistics of interest, i.e., the all-day evaporative fraction and the mid-day evaporative fraction, respectively. The parameter μ_d is the true mean of the difference between μ_1 and μ_2 , which is hypothesized to be equal to zero. The test statistic computed is

$$t = \frac{\hat{\mu}_d - 0}{\hat{\sigma}_d / \sqrt{n}} \quad (10)$$

where $\hat{\mu}_d$ is the computed mean difference between the all-day evaporative fraction and the mid-day evaporative fraction (an estimate of μ_d), $\hat{\sigma}_d$ is the sample standard deviation, n is the

number of observations, and 0 (zero) is the hypothesized value of μ_d . The computed value of the t statistic is compared to a t-critical value obtained from statistical tables for a level of significance α (Devore and Peck, 1986). The level of significance chosen for all tests was 0.05 (95% confidence level).

To test whether or not results were correlated with the characteristics of individual stations, each station was tested separately before testing the complete HAPEX-MOBILHY SAMER set of evaporative fraction statistics. The results of the paired-t tests for the general case are summarized in Table 4, and for the clear-sky case in Table 5. For general non-precipitation conditions, the mean mid-day evaporative fraction was statistically not equal to the mean all-day evaporative fraction for 7 of the 12 individual SAMER stations and for the experiment as a whole ($\alpha = 0.05$, p-value = 3.29×10^{-10}). For the clear-sky conditions, the mean mid-day evaporative fraction was statistically not equal to the mean all-day evaporative fraction for 10 of the 12 individual SAMER stations and for the experiment-wide case as well ($\alpha = 0.05$, p-value = 7.22×10^{-12}). The p-values for the experiment-wide tests provide very strong evidence against the null hypothesis that the two statistics are equal.

One reason why the mid-day and all-day mean evaporative fractions might differ would be the presence of water-limited conditions in afternoon periods, as illustrated in the conceptual drawing shown in Figure 8. Under this hypothesis, sufficient water would be available to sustain transpiration until early afternoon. After this point, the system would become water-limited and the latent heat flux would decline as a portion of the energy balance. Thus, the evaporative fraction measured at mid-day would be representative of the morning period, but not of the afternoon period. The mean all-day evaporative fraction would effectively average two different energy conditions represented by two different evaporative fraction values. This explanation is worth noting because such conditions are commonly observed in arid regimes and during dry seasons, although it was not very important in HAPEX-MOBILHY. The SOP was timed to coincide with the early part of the annual dry-down, a period with sufficient moisture to sustain transpiration throughout most days. A review of the HAPEX-MOBILHY data collection did reveal a few

examples of afternoon water-limiting conditions. Figure 9 shows the diurnal surface energy balance for one such case, at SAMER 11 (Fusterouau) on June 24, 1986. For this energy balance, the latent heat flux is predominant in the morning. After 1100 hours however, the sensible heat flux is predominant. In this case the evaporative fraction measured at mid-day is representative of the afternoon period rather than the morning, but the concept is the same as that illustrated by Figure 8; the evaporative fraction measured at mid-day is not representative of the activity for the all-day period.

Relationships Between Evaporative Fraction and Soil Moisture

Of particular interest in the study of remote sensing applications to surface hydrology is the relationship between soil moisture detectable by remote sensing and the partition of energy at the land surface. The surface energy balance Equation (1) is an expression of energy partition. The surface energy balance at a given time is subject to either an energy-limited state or a moisture-limited state. If plentiful moisture is available for the process of evapotranspiration, and if vapor pressure is low, water will be transported to the atmosphere to the maximum extent possible with the available energy (e.g., latent heat flux will approach the value of net radiation). On the other hand, if moisture is limited, the energy in excess of that required to transport water will appear as sensible and soil heat flux. The reduction of latent heat flux is therefore a function of water availability.

Research conducted in parallel to the evaporative fraction study presented in this paper provided soil moisture measurements for the first 5-cm depth of the Lubbon 1 site (SAMER 01) and the Castelnau site (SAMER 11) [Nichols, 1989a]. The Push Broom Microwave Radiometer (PBMR) used in the HAPEX-MOBILHY Program by the NASA C-130 remote sensing aircraft provided brightness temperature measurements. These values were converted to emissivity values which are linearly related to surface soil moisture. Because the correlation between sparse ground data and PBMR data was poor, the emissivity values could not be converted to soil

moisture values with confidence. Therefore, the emissivity values were treated as a soil moisture measurement for the purpose of examining the relation between remotely sensed soil moisture and surface energy partition.

Field-averaged emissivity values [Nichols, 1989a] were paired with mid-day evaporative fraction values for corresponding dates to explore the relationship between the two parameters. The resulting scatter plot is shown in Figure 10. No attempt was made to fit a regression line to the points in Figure 10 because no discernable pattern was present. Thus, we conclude that the surface soil moisture as measured with the PBMR was not linked in any fundamental way to the surface energy partition for these data. This is not an unexpected result for vegetated surfaces because the majority of water extraction for transpiration is from the deeper root zone rather than the thin surface layer observed by the PBMR.

To explore the relation between soil moisture for the profile as a whole and the surface energy partition, neutron probe soundings from the same SAMER sites (SAMER 01 and SAMER 10) [Goutorbe et al., 1989; Cuenca and Noilhan, 1990] were used to compute the relative water content, defined as

$$\Theta = \frac{\theta - \theta_{\min}}{\theta_{\max} - \theta_{\min}} \quad (11)$$

where θ is the average equivalent depth of soil moisture for the observed soil moisture profile at the time of interest (mm) and θ_{\min} and θ_{\max} are the minimum and maximum observed values of θ during the growing season, respectively. Use of the relative water content permitted direct comparison between soil profiles at different sites. The computed relative water content values for the SOP were paired with evaporative fraction values from the corresponding dates. The results are shown in Figure 11. A weak linear relationship is present ($r^2 = 0.40$) for the values shown in Figure 11. Because the linear model only explains 40% of the variation present, we cannot claim that these data demonstrate the underlying relationship between soil moisture at

depth and the surface energy partition. However, we do note that the profile soil moisture - evaporative fraction relationship is much more evident than the surface soil moisture - evaporative fraction relationship. From this it follows that the evaporative fraction over vegetated surfaces is more closely correlated to soil moisture at depth than to the surface layer observed by the PBMR sensor.

To quantify the relationship between moisture availability and the surface energy partition, we have contrasted soil moisture measurements with the evaporative fraction. Recall that unless soil moisture is a limiting condition it should not affect the surface energy partition. Hence, unless our database included water-stressed vegetation conditions, we should see no relationship in Figures 10 and 11. As noted previously, there were few examples of water-limiting conditions observed in the HAPEX-MOBILHY data collection.

Conclusions

A strong correlation between the mid-day and all-day mean evaporative fractions was demonstrated for clear-sky classified data using the HAPEX-MOBILHY SAMER database. The coefficient of regression (r^2) values for linear least-squares fits ranged from 0.82 to 0.99 for individual stations and $r^2 = 0.89$ for the full HAPEX-MOBILHY database. This correlation was in accordance with findings by FIFE researchers for Konza Prairie data. In addition, a strong correlation was also shown for more general conditions with r^2 ranging from 0.48 to 0.88 for individual stations and $r^2 = 0.80$ for the full experiment.

Application of the paired-t test resulted in a rejection in most cases of the hypothesis that the mid-day and all-day mean evaporative fraction values were equal (0.05-level test). On an experiment-wide basis, a p-value of 3.29×10^{-10} for the general case and 7.22×10^{-12} for the clear-sky case provided very strong evidence against the equality hypothesis. Therefore, the all-day and mid-day evaporative fraction variables are highly correlated, but not equal.

The relationships between the evaporative fraction and soil moisture monitored by remote- and ground-based measurement systems were examined. There was no discernable relationship between soil moisture in the thin surface layer observed by passive microwave remote sensing sensors and the surface energy partition represented by the evaporative fraction statistic. A weak linear relationship ($r^2 = 0.40$) was shown to exist between the soil moisture over the entire root zone and the evaporative fraction. Because the HAPEX-MOBILHY data could be characterized as generally energy-limited, rather than water-limited, no strong relationship between available moisture and the surface energy partition was expected.

Acknowledgments

This research was supported by USDA-ARS Specific Cooperative Agreement Number 58-3K47-9-006, "Water Budget Studies With HAPEX-MOBILHY." Additional publication support was provided by Pacific Northwest Laboratory, operated for the U.S. Department of Energy by Battelle Memorial Institute under Contract DE-AC06-76RLO 1830.

References

- André, J. C., J.-P. Goutorbe, and A. Perrier, HAPEX-MOBILHY: a hydrological atmospheric experiment for the study of water budget and evapotranspiration at the climatic scale, Bull. Meteorol. Soc., **67**, 134-144, 1986.
- André, J. C., J.-P. Goutorbe, A. Perrier, F. Becker, P. Bessemoulin, P. Bougeault, Y. Brunet, W. Brutsaert, T. Carlson, R. Cuenca, J. Gash, J. Gelpe, P. Hildebrand, J. P. Lagouarde, C. Lloyd, L. Mahrt, P. Mascart, C. Mazaudier, J. Noilhan, C. Ottlé, M. Payen, T. Phulpin, R. Stull, J. Shuttleworth, T. Schmugge, O. Taconet, C. Tarrieu, R. M. Thepenier, C. Valencogne, D. Vidal-Madjar, and A. Weill, First results from HAPEX-MOBILHY Special Observing Period, Ann. Geophysicae, **5**, 477-492, 1988.
- Bessemoulin, P. G., G. Desroziers, M. Payen, and C. Tarrieu, Atlas des donnees SAMER, 256 pp., Centre National de Recherches Météorologiques Report. Toulouse, France, 1987.
- Cuenca, R. H., and J. Noilhan, Use of soil moisture measurements in hydrologic balance studies, in Land Surface Evaporation Fluxes: Their Measurement and Parameterization, edited by T. J. Schmugge and J. C. André, Springer-Verlag, New York, 1990.
- Devore, J. and R. Peck, Statistics: The Exploration and Analysis of Data, 699 pp., West Publishing Company, St. Paul, Minnesota, 1986.
- Goutorbe, J.-P., A critical assessment of the SAMER network accuracy, Land Surface Evaporation Fluxes: Their Measurement and Parameterization, edited by T. J. Schmugge and J. C. André, Springer-Verlag, New York, 1990.
- Goutorbe, J.-P., J. Noilhan, C. Valencogne, and R. H. Cuenca, Soil moisture variations during HAPEX-MOBILHY, Ann. Geophysicae, **7(4)**, 415-426, 1989.
- Itier, B., Une méthode simplifiée pour la mesure du flux de chaleur sensible, Journal de Recherches Atmosphériques, **14**, 17-34, 1980.
- Itier, B., Révision d'une méthode simplifiée pour la mesure du flux de chaleur sensible, Journal de Recherches Atmosphériques, **16**, 85-90, 1982.

- Marre, J. L., and J. P. Goutorbe, Analyse du rayonnement, période d'observation intensive, experience in HAPEX-MOBILHY, Centre National de Recherches Météorologiques Report, Toulouse, France, 1988.
- Nichols, W. E., Land surface energy balance and surface soil moisture variation in HAPEX-MOBILHY, M.S. thesis, 162 pp., Oregon State Univ., Corvallis, Oregon, 1989a.
- Nichols, W. E., SAMTRAN version 3.5 user's guide, Report No. 101, Department of Bioresource Engineering, Oregon State Univ., Corvallis, Oregon, 1989b.
- Thompson, N., I. A. Barrie, and M. Ayles, The meteorological office rainfall and evaporation calculation system: MORECS, Hydrological Memorandum No. 45, Meteorological Office, London, 69pp., 1981.
- Riou, C., Une expression analytique du flux de chaleur sensible en conditions suradiabatiques à partir de mesures du vent et de la température à deux niveaux, Journal de Recherches Atmosphériques, 16, 15-22, 1982.
- Sellers, P. J., J. L. Dorman, C. Walthall, F. G. Hall, D. E. Strebel, B. L. Markham, J. R. Wang, R. D. Kelly, S. B. Verma, B. L. Blad, D. S. Schimel, R. Grossman, W. Brutsaert, R. Desjardins, L. Fritschen, R. Frouin, E. Kanemasu, and I. McPherson, First ISLSCP Field Experiment: experiment execution and preliminary analyses, in Remote Sensing and Large-Scale Global Processes, Proc. IAHS Third Int. Assembly, Baltimore, Maryland, May 1989, IAHS Publ. 186, pp.49-58, edited by A. Rango, 1989.
- Shuttleworth, W. J., R. J. Gurney, A. Y. Hsu, and J. P. Ormsby, FIFE: the variation in energy partition at surface flux sites, in Remote Sensing and Large-Scale Global Processes, Proc. of the IAHS Third Int. Assembly, Baltimore, Maryland, May 1989, IAHS Publ. 186, pp.67-74, edited by A. Rango, 1989.
- Weisberg, S., Applied Linear Regression, 324 pp., John Wiley and Sons, New York, 1985.

Author Address List

R. H. Cuenca, Department of Bioresource Engineering, Gilmore Hall, Oregon State University, Corvallis, OR 97331-3906. Telephone (503) 737-2041.

W. E. Nichols, Geosciences Department, Pacific Northwest Laboratory, P.O. Box 999 MSIN K6-77, Richland, WA 99352. Telephone (509) 376-8247, FTS 444-8247. Facsimile (509) 376-4428, Verification (509) 376-4686.

Figure Captions

Fig. 1. Distribution of SAMER surface energy balance measurement stations in the HAPEX-MOBILHY experiment grid, and location of the HAPEX-MOBILHY experiment grid in southwest France.

Fig. 2. Diurnal surface energy balance on June 16, 1986, measured by SAMER 01 (Lubbon 1) over a mature oat crop canopy (m.d. indicates missing data due to instrument failure).

Fig. 3. Diurnal surface energy balance on June 16, 1986, measured by SAMER 05 (Lubbon 2) over a young maize crop canopy.

Fig. 4. Daylight evaporative fraction for the surface energy balances shown in Figures 2 and 3 on June 16, 1986. Local daylight period and mid-day period (11:00 to 13:00 hours LT) are indicated.

Fig. 5. Diurnal surface energy balance on June 4, 1986, measured by SAMER 11 (Fusterouau) over a young maize crop canopy.

Fig. 6. Scatter plots of mid-day evaporative fraction versus all-day evaporative fraction by SAMER station for the "clear-sky" and "non-clear-sky" data sets. The 1:1 line and the least-squares linear regression fit are shown for each. (a) SAMER 01. (b) SAMER 02. (c) SAMER 03. (d) SAMER 04. (e) SAMER 05. (f) SAMER 06. (g) SAMER 07. (h) SAMER 08. (i) SAMER 09. (j) SAMER 10. (k) SAMER 11. (l) SAMER 12.

Fig. 7. Scatter plot of mid-day evaporative fraction versus all-day evaporative fraction for the "clear-sky" data set for all 12 SAMER stations. The 1:1 line and the least squares linear regression fit are shown.

Fig. 8. Idealized diurnal latent heat flux illustrating energy-limited and afternoon-moisture-limited conditions. The evaporative fraction measured at mid-day under afternoon-moisture-limited conditions would not be representative of the all-day evaporative fraction.

Fig. 9. Diurnal surface energy balance on June 24, 1986, measured by SAMER 11 (Fusterouau) over a young maize crop canopy. This energy balance shows an example of afternoon-moisture-limited conditions.

Fig. 10. Scatter plot of emissivity versus mid-day evaporative fraction for data from SAMER stations 01 (Lubbon 1) and 10 (Castelnau). Emissivity is linearly related to soil moisture in the 0-cm to 5-cm-depth range of the soil.

Fig. 11. Scatter plot of relative water content (Θ) versus mid-day evaporative fraction. The relative water content represents soil moisture content for the complete root zone.

TABLE 1. SAMER Stations [modified from Bessemoulin et al., 1987]

SAMER	Site Name	Latitude	Longitude	Elev. (m)	Soil Texture (%)			Crop	Irrigated
					Cl	Si	Sa		
01	Lubbon	44°07'N	0°03'W	146	2	5	93	Oats	No
02	Casteljaloux	44°19'N	0°07'E	131	35	49	16	Maize	Yes
03	Caumont	43°41'N	0°07'W	113	17	46	37	Soybeans	No
04	Courrensan	43°49'N	0°16'E	148	-	-	-	Wheat	No
05	Lubbon 2	44°07'N	0°03'W	146	1	2	97	Maize	Yes
06	Sabres	44°05'N	0°50'W	81	3	1	96	Maize	Yes
07	Bats	43°38'N	0°26'W	144	18	51	31	Maize	No
08	Vicq	43°46'N	0°51'W	15	10	16	74	Maize	Yes
09	Tieste	43°32'N	0°02'E	145	12	61	27	Maize	Yes
10	Castelnau	43°35'N	0°03'W	239	11	66	23	Maize	No
11	Fusterouau	43°42'N	0°01'W	146	20	34	46	Maize	Yes
12	Lagrange	43°58'N	0°03'W	152	-	-	-	Maize	Yes

Cl, clay; Si, silt; Sa, sand

TABLE 2. SAMER Station Measurements [modified from Goutorbe, 1988]

MEASUREMENT	INSTRUMENT
BASIC MEASUREMENTS	
- Net Radiation	CROUZET net radiometer (0.3 to 50 μm)
- Soil Heat Flux	Thornwaite flux-meter
- Temperature Difference	6 copper-constantan thermocouples in 2 probes*
- Wind Speed Difference	2 MCB anemometers*
OTHER MEASUREMENTS	
- Air Temperature	Platinum wire (precision = 0.1 $^{\circ}\text{C}$)
- Air Humidity	SPSI capacity sensor (estimated precision = 5%)
- Precipitation	Precis Mecanique tipping bucket rain gage
- Radiation	4 SCHENCK radiometers: <ul style="list-style-type: none"> - shortwave upward (0.3 to 3.0 μm) - shortwave downward (0.3 to 3.0 μm) - total upward (0.3 to 60 μm) - total downward (0.3 to 60 μm)

* Temperature and wind speed probes installed 1.5-m apart

TABLE 3. Linear Regression Statistics for Mid-day Evaporative Fraction Versus All-day Evaporative Fraction

SAMER	General Case				Clear Sky			
	Number	n	β_1	β_0	r^2	n	β_1	β_0
01	41	0.942	-0.029	0.882	7	0.848	0.026	0.994
02	41	0.735	0.156	0.817	10	1.022	-0.085	0.941
03	39	0.720	0.148	0.659	6	1.683	-0.679	0.942
04	49	0.656	0.153	0.835	10	0.707	0.142	0.909
05	37	0.776	0.084	0.480	7	1.027	-0.150	0.851
06	34	0.841	0.072	0.715	3	0.897	-0.012	0.997
07	42	0.892	0.055	0.676	9	0.987	-0.065	0.901
08	27	1.223	-0.199	0.673	8	1.384	-0.322	0.872
09	39	0.666	0.209	0.522	8	1.265	-0.326	0.817
10	35	1.056	-0.106	0.573	6	1.801	-0.637	0.948
11	37	0.683	0.135	0.750	9	1.171	-0.204	0.839
12	32	0.853	0.063	0.695	8	0.762	0.048	0.832
ALL	453	0.811	0.087	0.802	91	0.856	0.025	0.887

Here, n, number of observations; β_1 , slope of regression line, β_0 , intercept of regression line, r^2 , coefficient of determination.

TABLE 4. Summary of Paired-t Tests For Hypothesis About μ_d For General Conditions

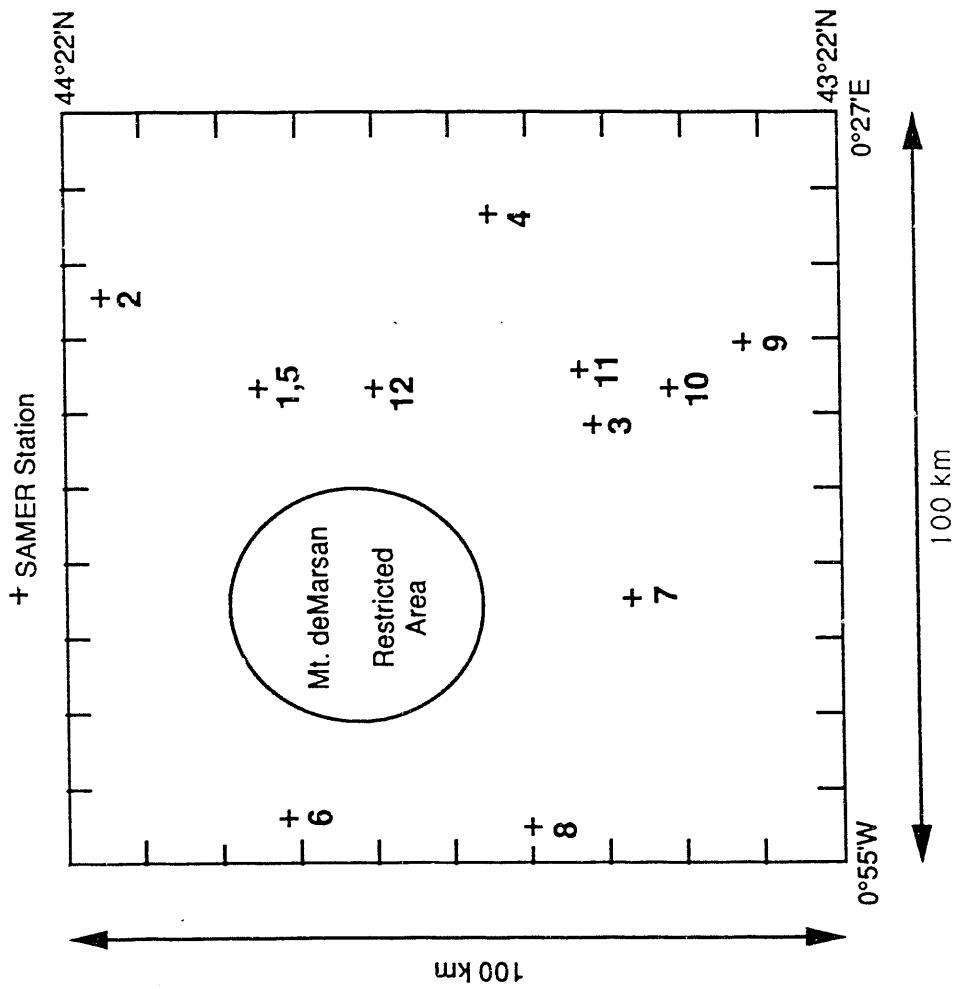
SAMER	n	$\hat{\mu}_d$	$\hat{\sigma}_d^2$	$\hat{\sigma}_d$	t	p-value	Reject?
01	41	-0.0762	1.0105	0.102	-4.77	0.0000249	Yes
02	41	0.0162	4.00444	0.0666	1.55	0.128	No
03	39	0.0762	8.00862	0.0929	5.13	0.00000892	Yes
04	49	0.0162	1.0147	0.0121	0.934	0.354	No
05	37	0.0895	9.00941	0.0970	5.61	0.00000229	Yes
06	34	0.00641	8.00873	0.0934	0.400	0.692	No
07	42	0.0199	5.00515	0.0718	1.80	0.0795	No
08	27	0.0139	7.00742	0.0861	0.841	0.408	No
09	39	0.0577	5.00552	0.0743	4.85	0.0000212	Yes
10	35	0.0645	5.00525	0.0724	5.27	0.00000775	Yes
11	37	0.0488	7.00766	0.0875	3.39	0.00170	Yes
12	32	0.0312	6.00693	0.0832	2.12	0.0418	Yes
ALL	453	0.0295	0.00962	0.0981	6.40	3.29 x 10 ⁻¹⁰	Yes

Here, n, number of samples; $\hat{\mu}_d$, mean value of difference between mid-day and all-day evaporative fraction; $\hat{\sigma}_d^2$ variance; $\hat{\sigma}_d$, standard deviation; t, test statistic; p-value, smallest level of significance at which H_0 would be rejected.

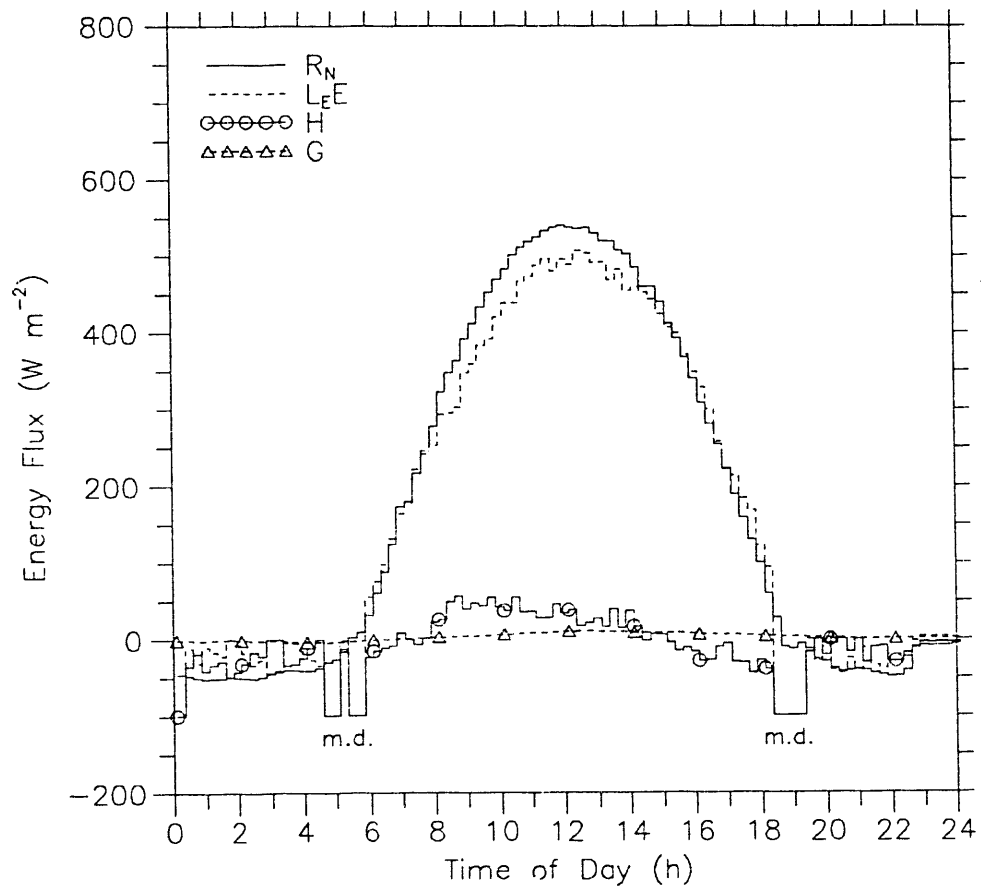
TABLE 5. Summary of Paired-t Tests For Hypothesis About μ_d For "Clear-Sky" Conditions

SAMER	n	$\hat{\mu}_d$	$\hat{\sigma}_d^2$	$\hat{\sigma}_d$	t	p-value	Reject?
01	7	-0.0831	0.00223	0.0473	-4.65	0.00350	Yes
02	10	0.0691	0.00102	0.0320	6.84	0.0000757	Yes
03	6	0.0932	0.0932	0.0394	5.79	0.00216	Yes
04	10	-0.0128	0.00841	0.0917	-0.441	0.669	No
05	7	0.128	0.000761	0.0276	12.2	0.0000182	Yes
06	3	0.0887	0.0000605	0.00778	19.8	0.00255	Yes
07	9	0.0729	0.00247	0.0497	4.40	0.00228	Yes
08	8	0.0286	0.00508	0.0713	1.13	0.294	No
09	8	0.107	0.00245	0.0495	6.12	0.000481	Yes
10	6	0.0896	0.00268	0.0517	4.24	0.00813	Yes
11	9	0.0987	0.00218	0.0467	6.34	0.000224	Yes
12	8	0.111	0.00141	0.0376	8.37	0.0000683	Yes
ALL	91	0.0633	0.00586	0.0766	7.88	7.22×10^{-12}	Yes

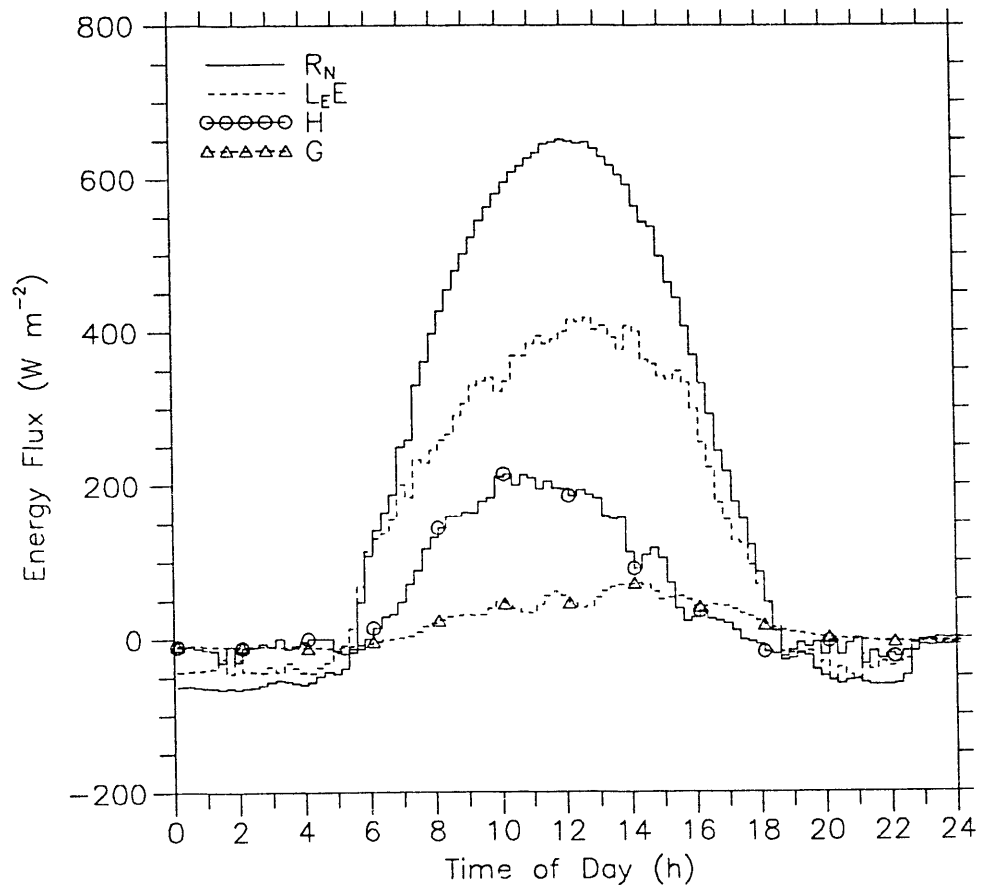
Here, n, number of samples; $\hat{\mu}_d$, mean value of difference between mid-day and all-day evaporative fraction; $\hat{\sigma}_d^2$ variance; $\hat{\sigma}_d$, standard deviation; t, test statistic; p-value, smallest level of significance at which H_0 would be rejected.



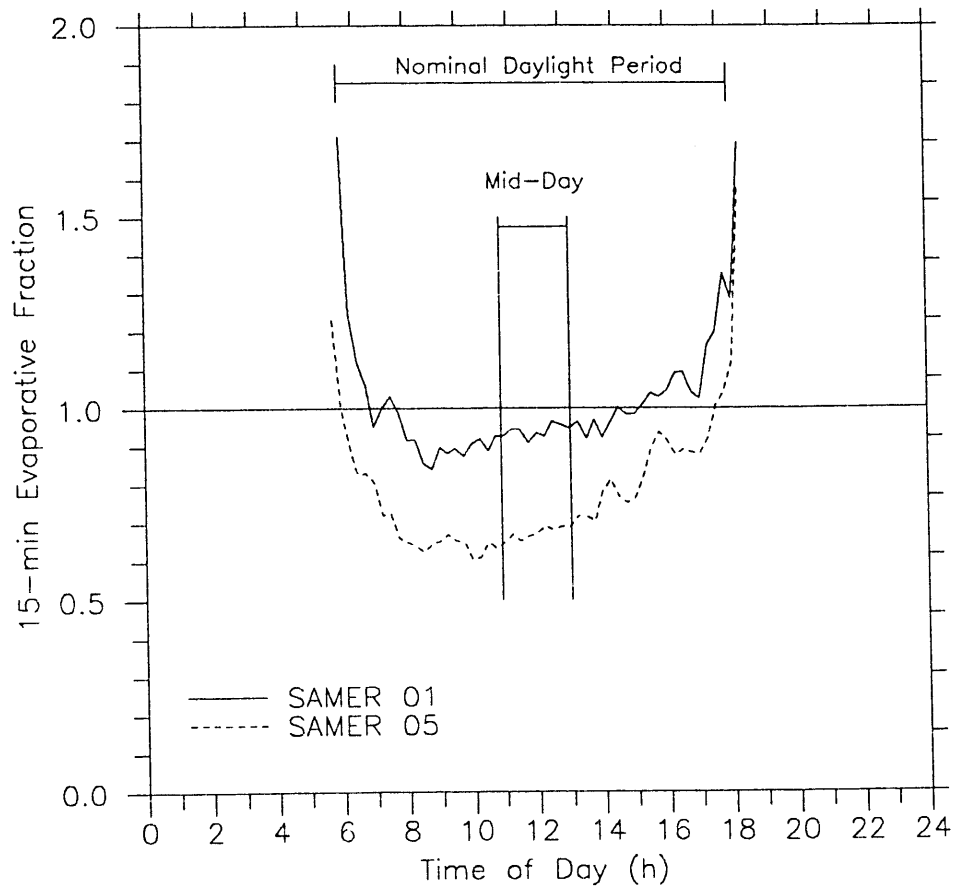
HAPEX-MOBILHY SAMER 01 June 16, 1986



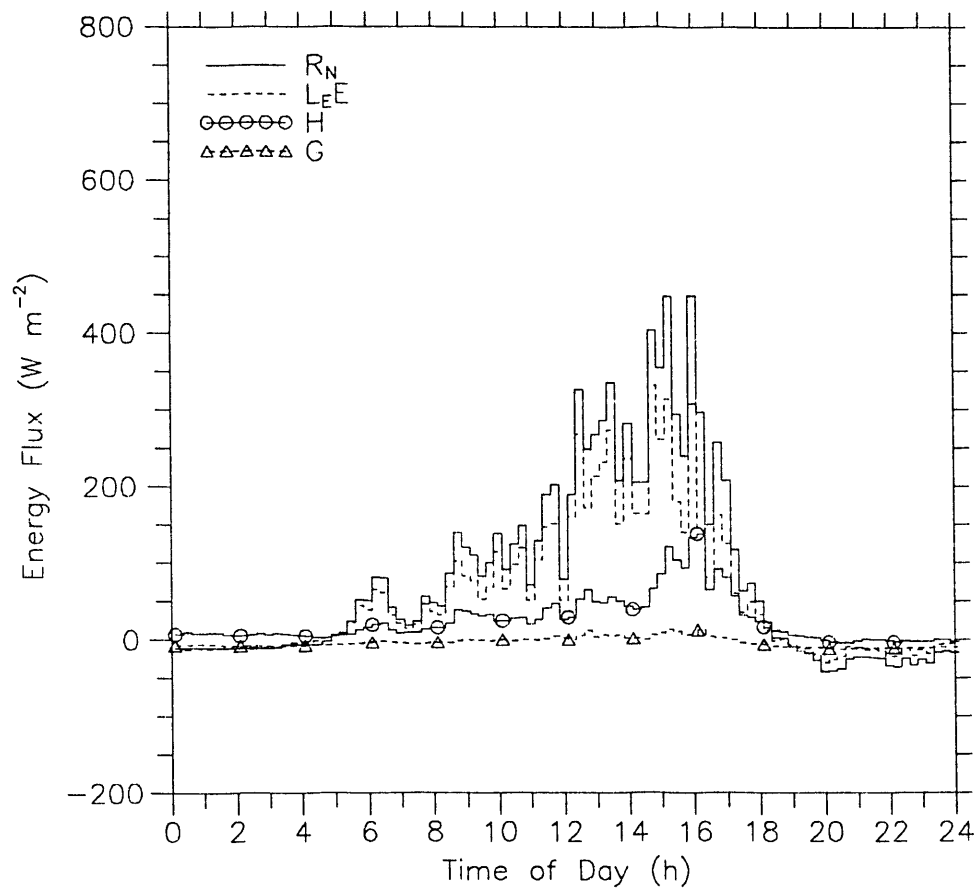
HAPEX-MOBILHY SAMER 05 June 16, 1986

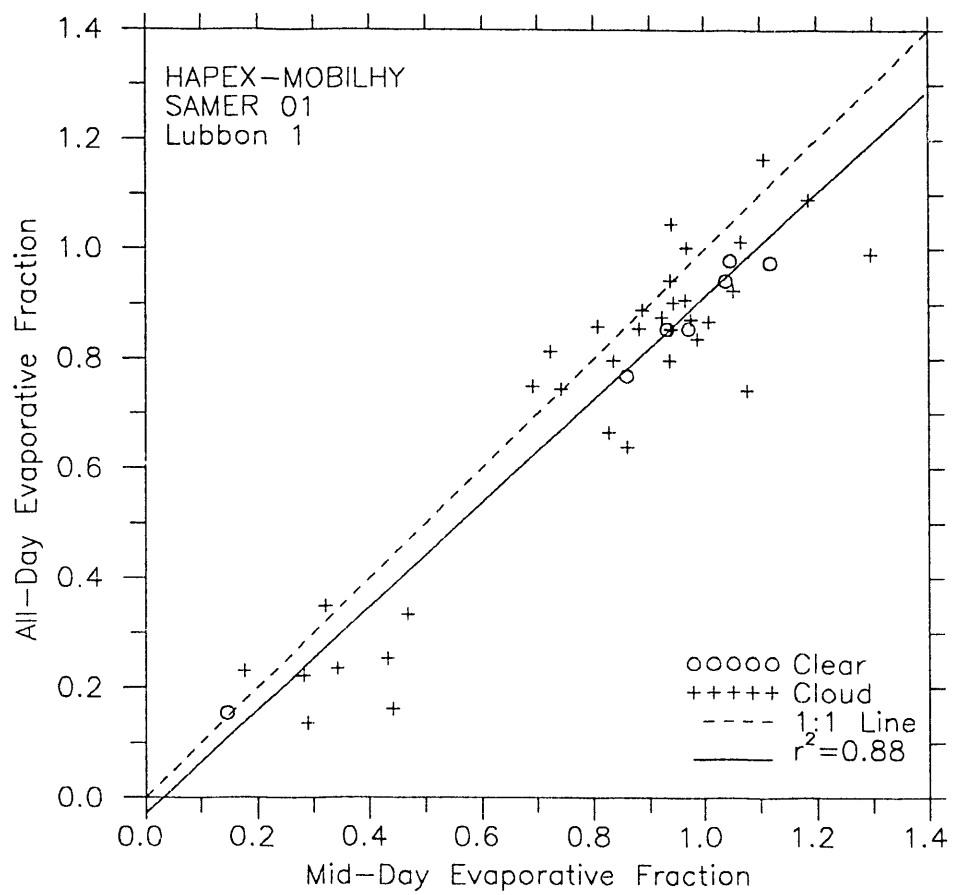


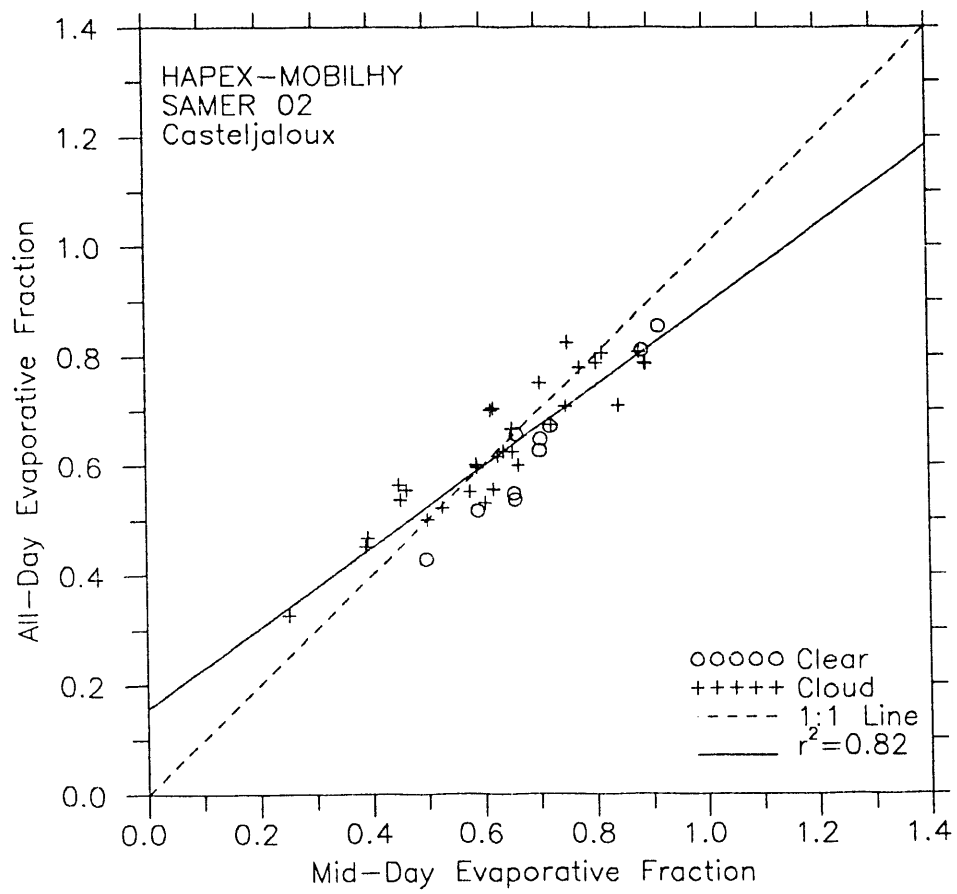
HAPEX-MOBILHY SAMER 01, 05 June 16, 1986

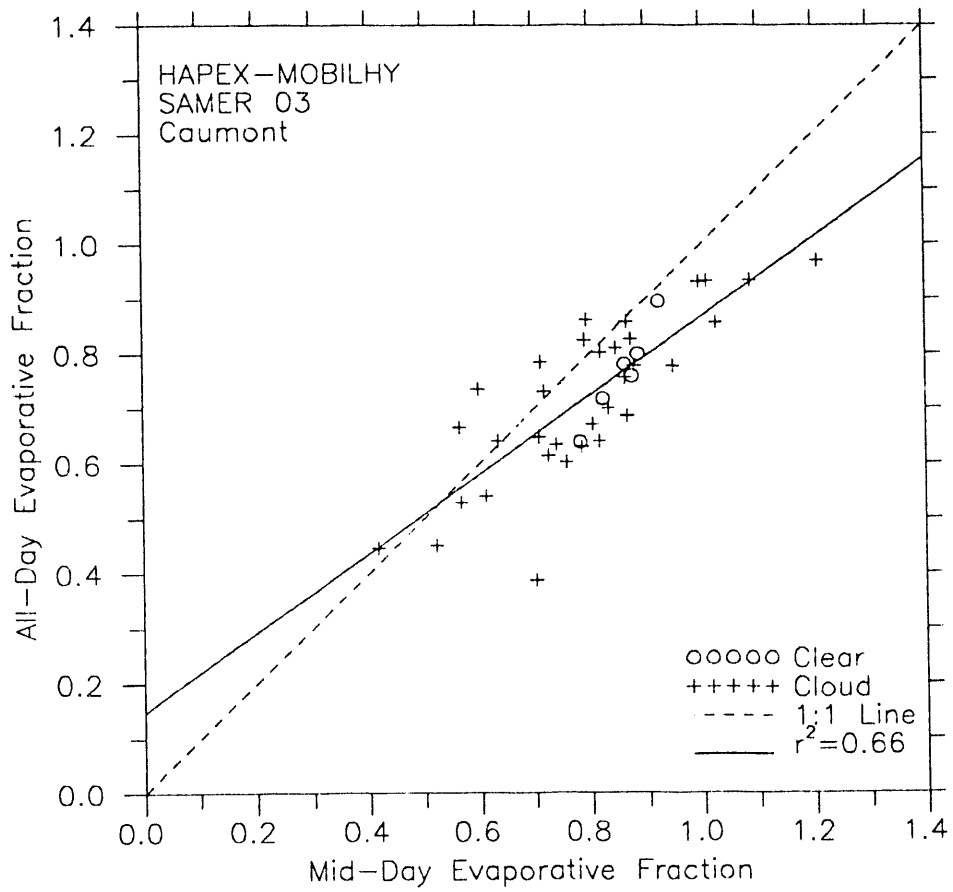


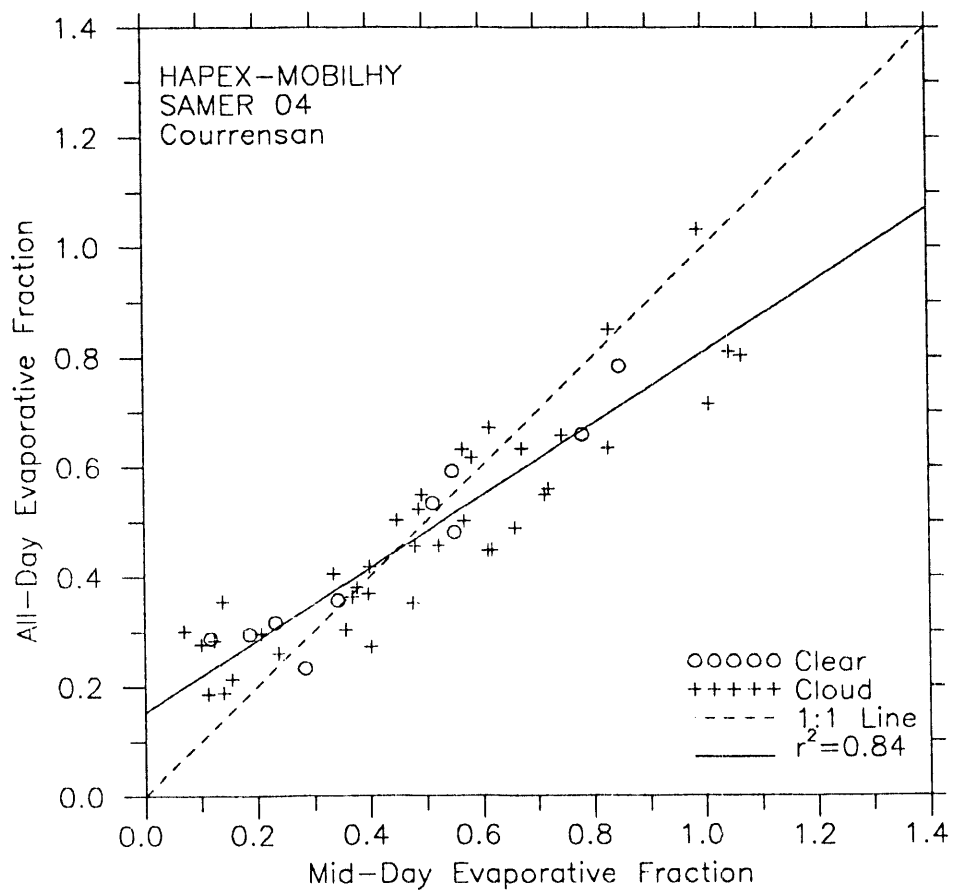
HAPEX-MOBILHY SAMER 11 June 4, 1986

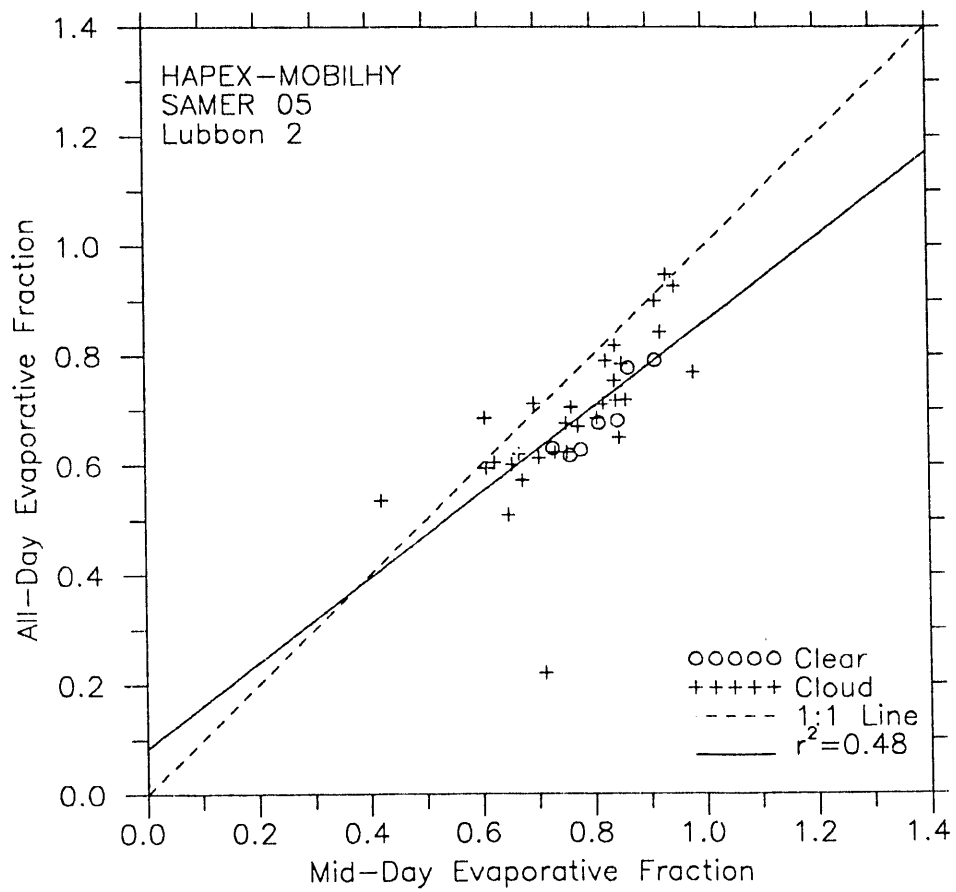


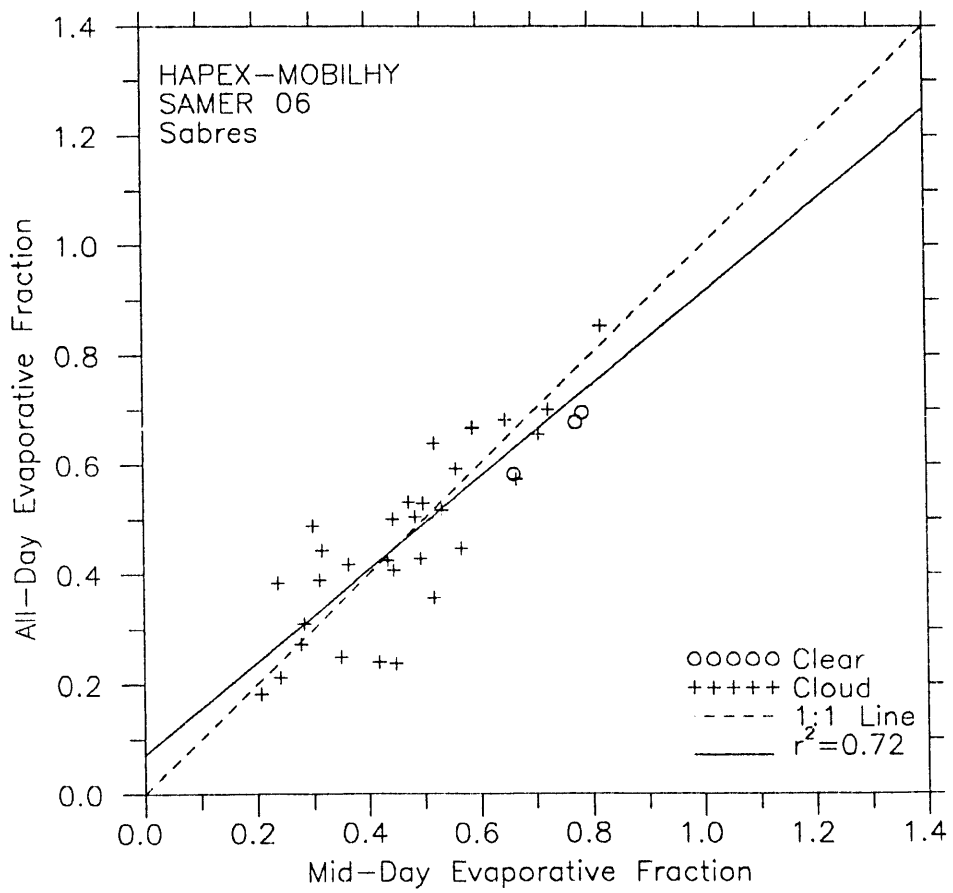


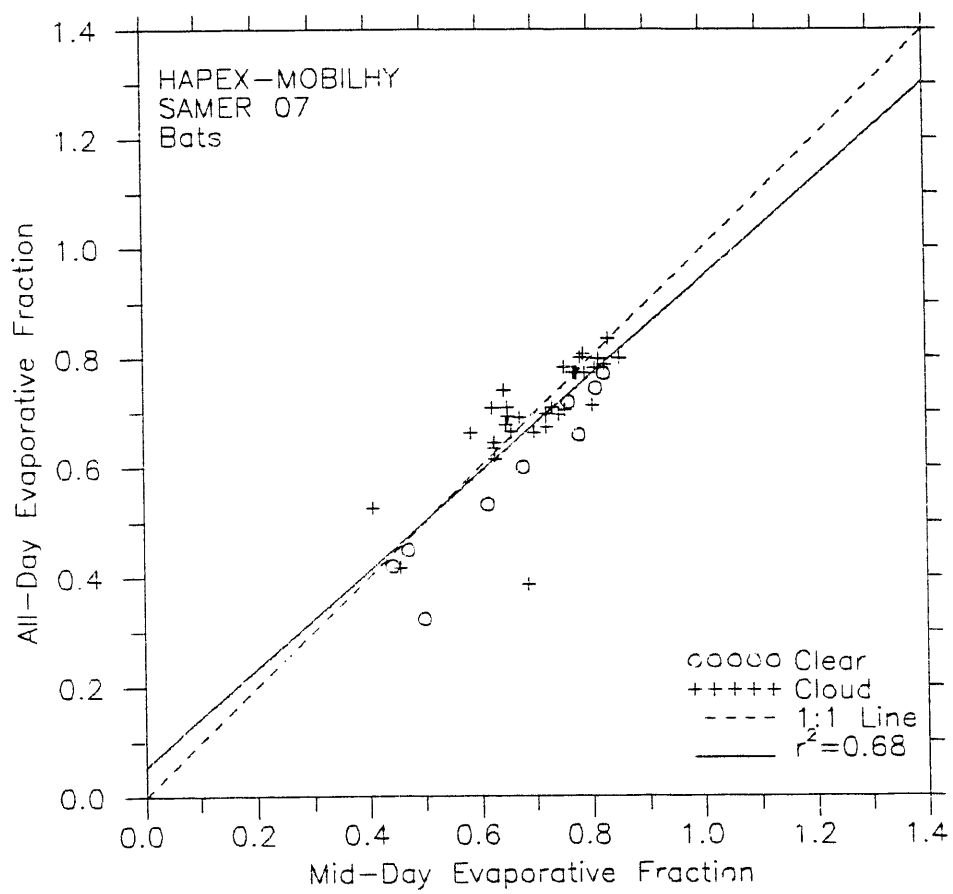


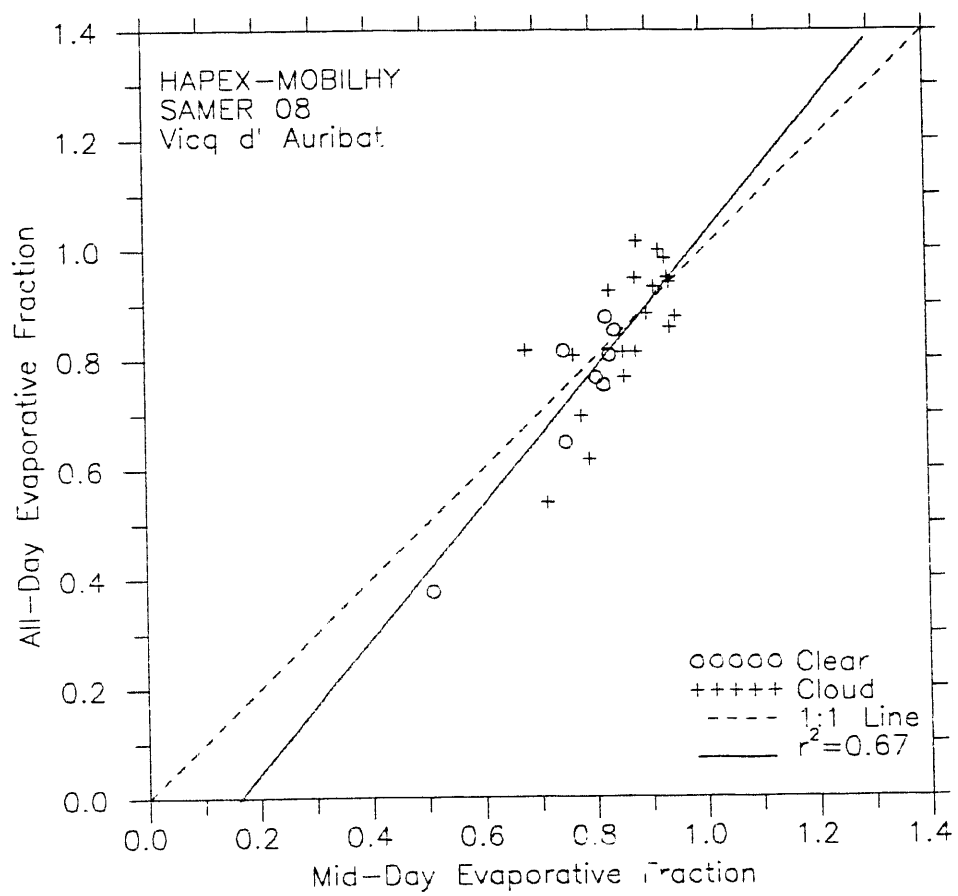


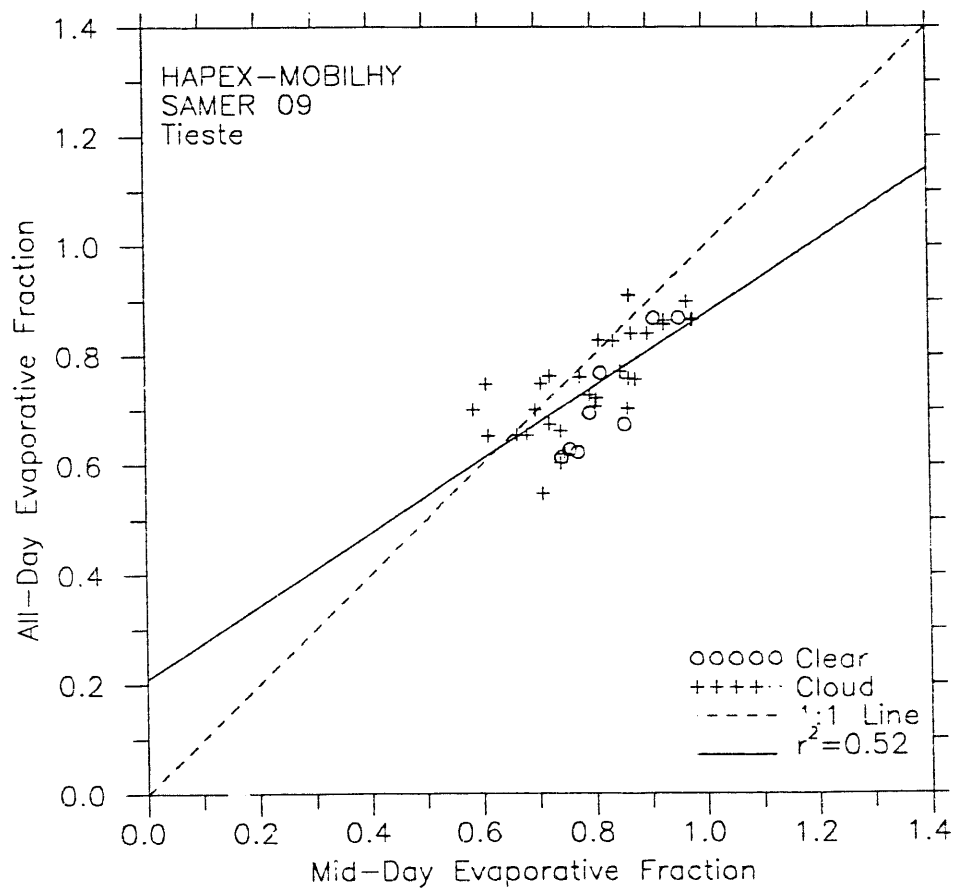


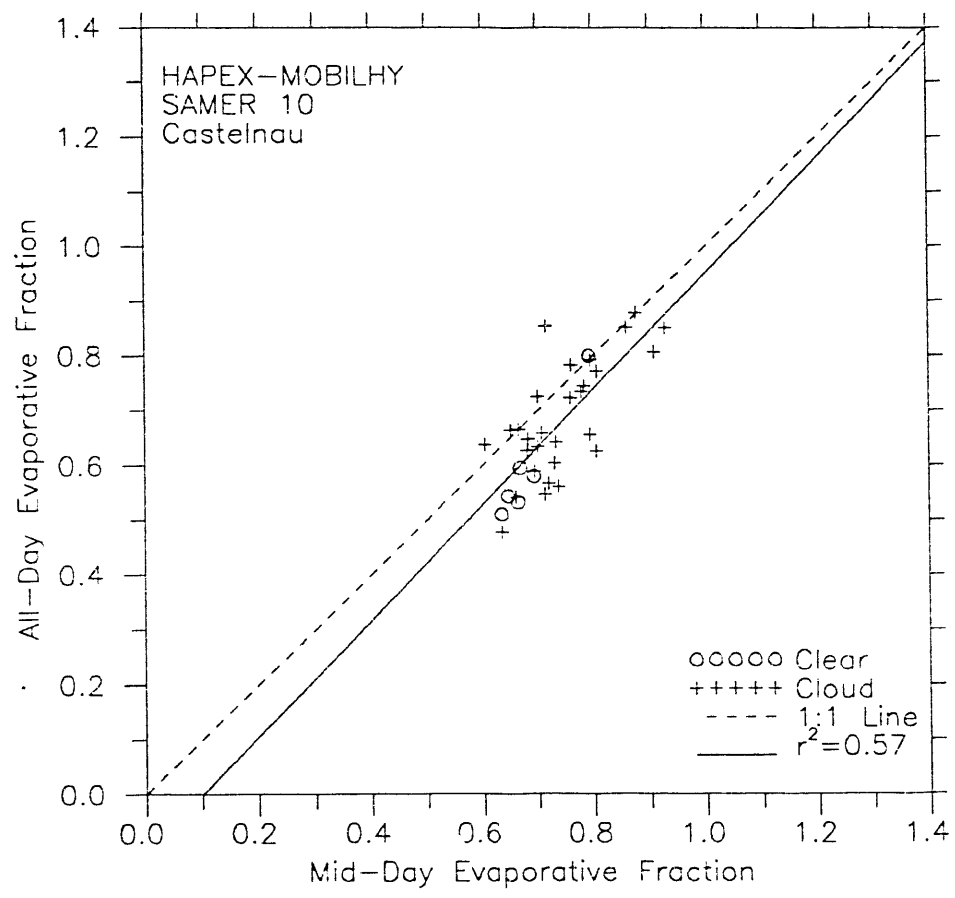


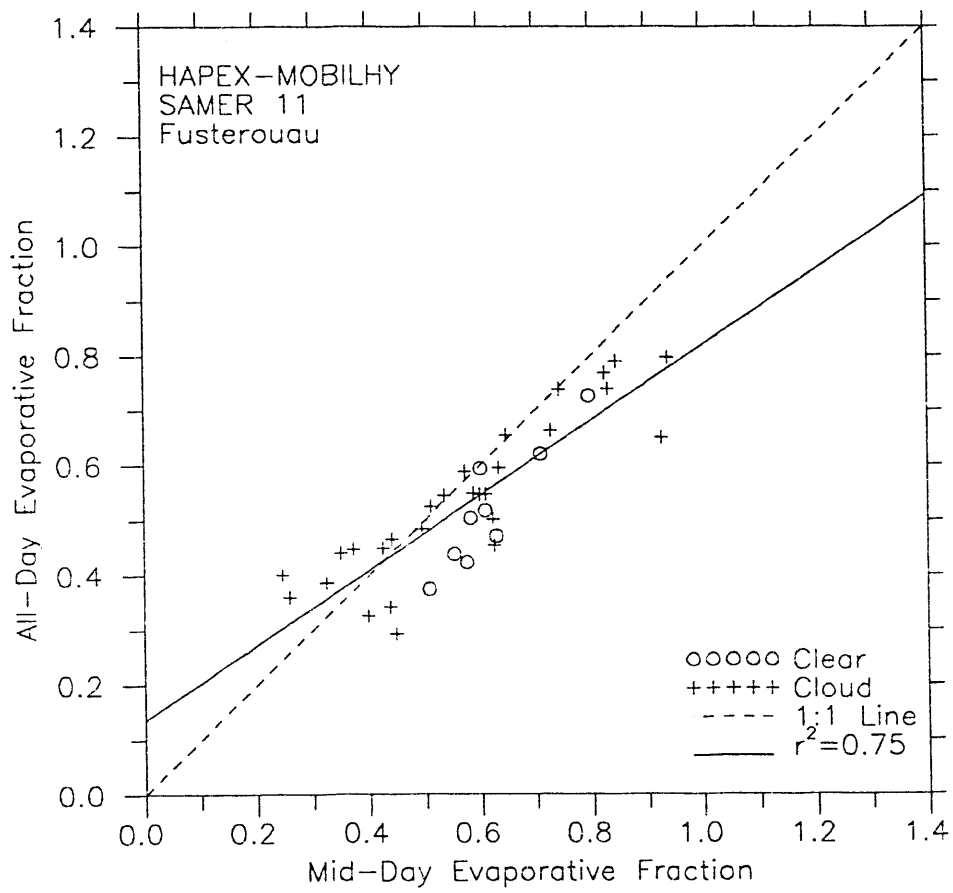


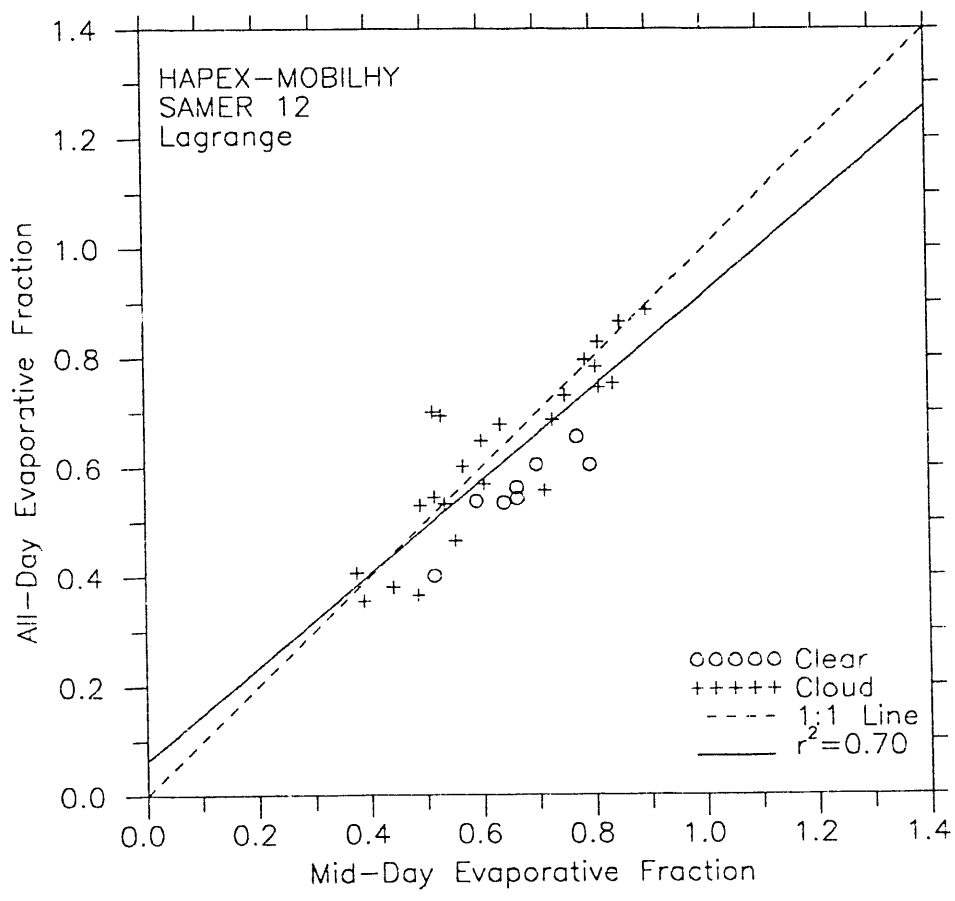


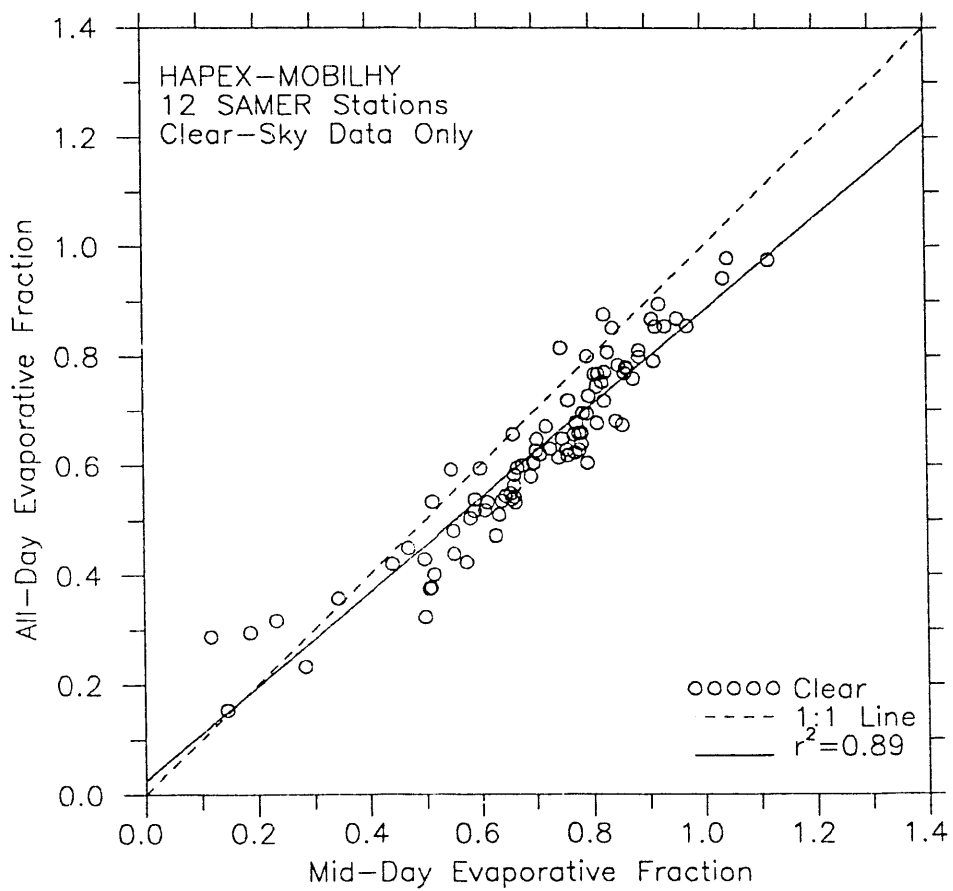




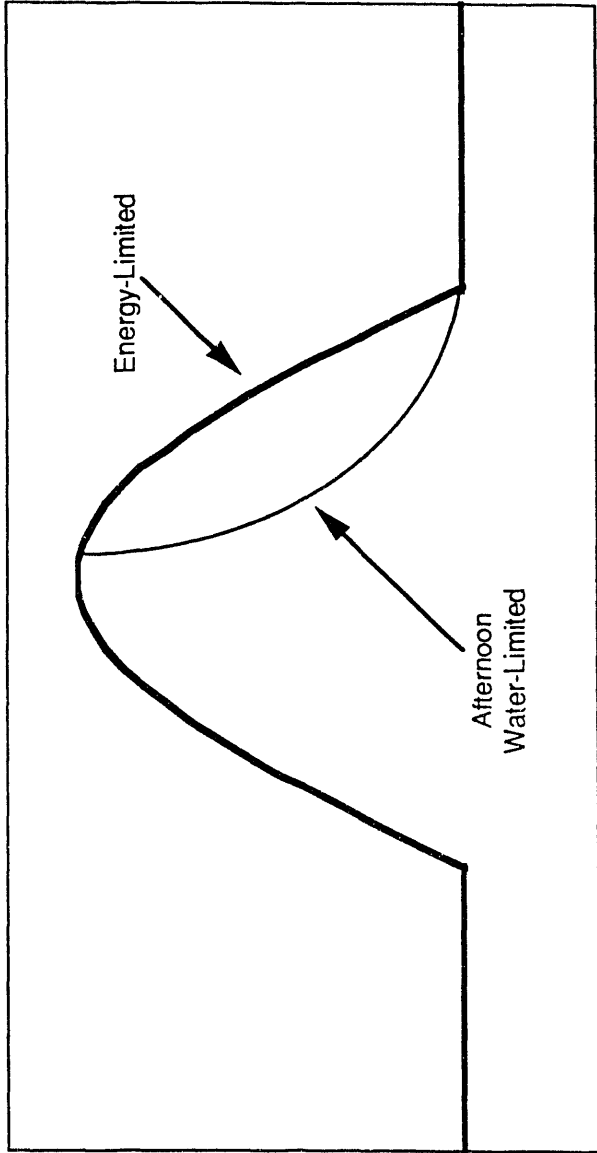








Latent Heat Flux (λE)



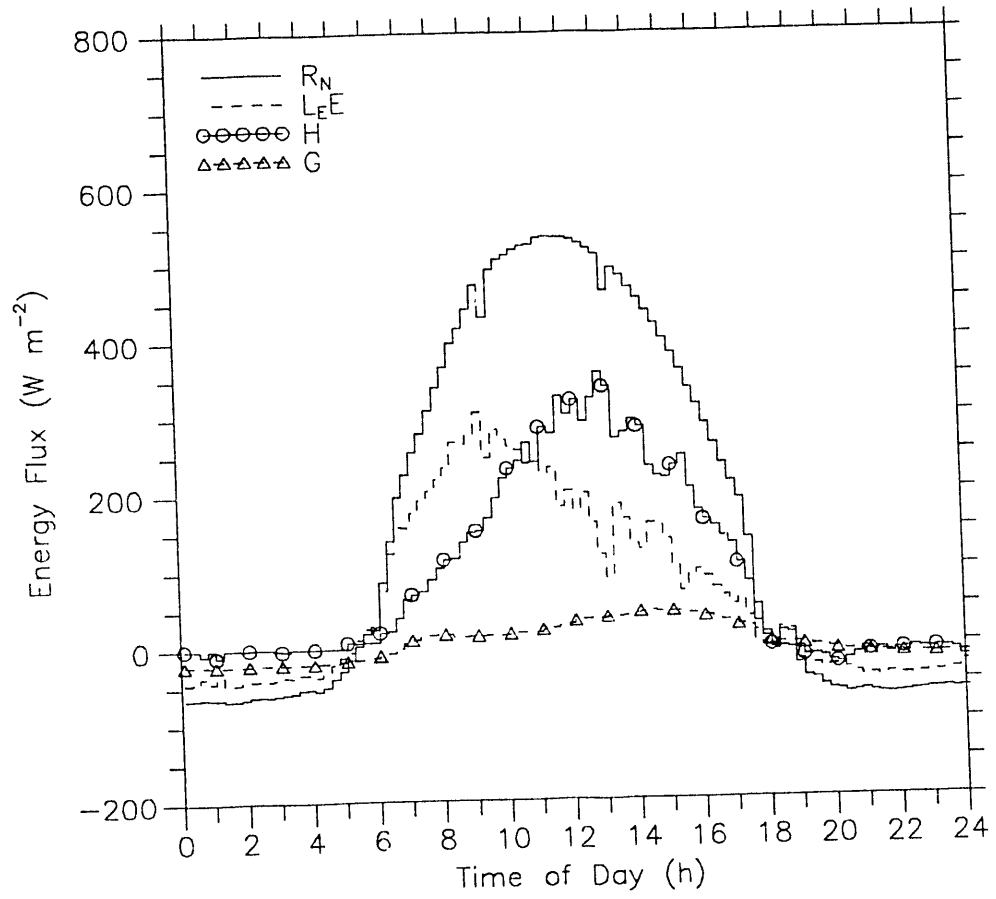
SUNSET

SOLAR NOON

SUNRISE

Time of Day

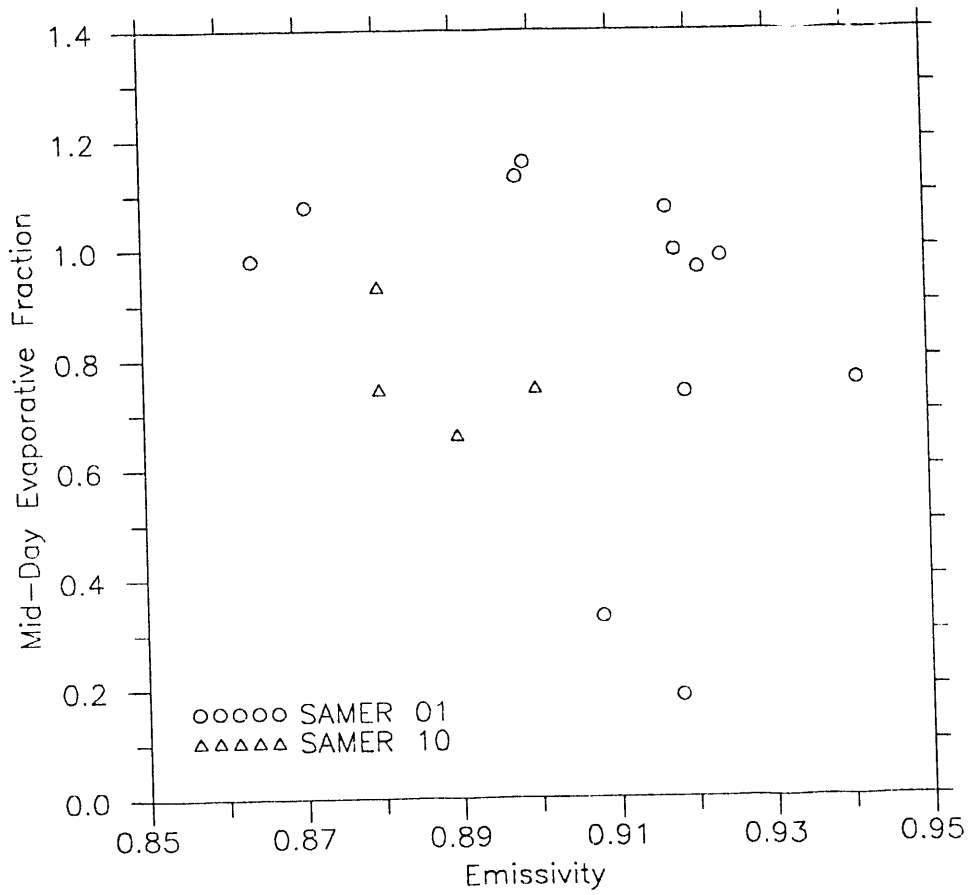
HAPEX--MOBILHY SAMER 11 June 24, 1986



HAPEX-MOBILHY

SAMER 01, 10

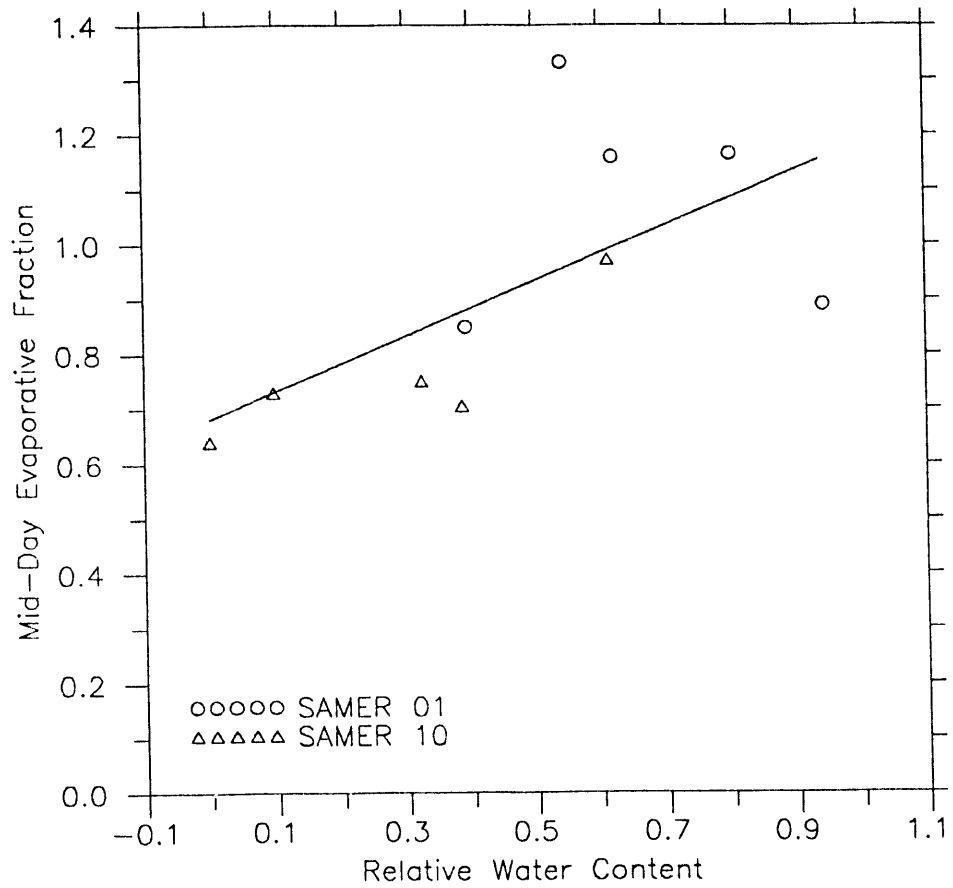
SOP



HAPEX-MOBILHY

SAMER 01, 10

SOP



**DATE
FILMED
4 129 192**

